A low-cost system and calibration method for veiling luminance measurement

Stefano Cattini, Costantino Grana, Rita Cucchiara, and Luigi Rovati
Department of Information Engineering, University of Modena and Reggio Emilia
Via Vignolese 905/b, I-41125, Modena, Italy
Email: stefano.cattini@unimore.it

***Abstract*—A CCD-based measuring instrument aimed at the veiling luminance estimation and the relative low-cost calibration method are described. The system may allow the estimation of the optimum luminance levels in road-tunnels lighting, thus both increasing the drivers safety and avoiding energy wasting hence unjustified higher lighting-costs.**

I. Introduction

"The aim of tunnel lighting is to ensure that users, both during the day and by night, can approach, pass through, and exit the tunnel without changing direction or speed with the degree of safety commensurate to that on the approach road" [1].
In tunnels lighting, the threshold zone lighting – the lighting of the first part of the tunnel, directly after the portal – plays a key role in traffic safety being the lighting of the threshold zone of the tunnel which allows drivers to see into the tunnel whilst in the access zone, thus avoiding drivers experiencing the hazardous "black hole" effect. As a result, the tunnel lighting has to adapt to the external lighting level, hence, the minimum access-zone luminance varies with changes in day-light conditions. Therefore, during the day, the luminance levels in the threshold and transition zones need to be constant percentages of the luminance in the access zone. Higher access-zone luminance level will results in energy wasting and higher costs and may lead to the driver dazzle too. Therefore, it is necessary to provide automatic control of the artificial lighting in these zones.

Standards and recommendations of European Commission, PIARC and other professional bodies of the European Union define minimal technological requirements for equipment and operation of the tunnels in scope of Trans-European Road Network. Italian tunnel lighting is regulated by the UNI 11095 national standard [2]. In accordance with CIE 88-1990 [3], daytime lighting requirements of long tunnels may be determined from the estimation of the veiling luminance L_v.

In this paper, we propose to use a camera system connected to a personal computer in order to estimate the veiling luminance. The developed measuring system has been calibrated by using a luminance standard realized exploiting a reflectance standard illuminated by a xenon lamp.
After a brief review of both the tunnel-lighting normative context (section II) and theoretical background (section III), the developed measuring system and calibration method will be presented in sections IV and V respectivelly. Then, calibration results demonstrating the applicability of the proposed calibration method are reported in subsection V-B and conclusion are drawn in section VI.

II. The normative context

In daylight condition, it is essential to know the luminance in the access zone of the tunnel in order to verify if the standard recommendations are respected. As previously stated, Italian tunnel lighting is regulated by the UNI 11095 national standard [2]. From UNI 11095, the required luminance levels in the entrance zone of the tunnel may be determined from the estimation of the veiling luminance L_v [2]:

$$L_v = L_{seq} + L_{atm} + L_{winds} \ . \tag{1}$$

where:

- L_{seq}: equivalent veiling luminance as a result of the straylight in the optical media of the visual system;
- L_{atm}: veiling luminance as a result of the straylight in the atmosphere;
- L_{winds}: veiling luminance as a result of the light scattered in the vehicle windscreen.

The UNI 11095 standard defines also the measurement procedure for the L_{seq}, L_{atm} and L_{winds} estimation.

The windscreen veiling luminance L_{wind} could be directly estimated from the L_{seq} [2]:

$$L_{wind} = 0.4 \cdot L_{seq} \ , \tag{2}$$

The atmospheric veiling luminance L_{atm}, could be estimated as [2]:

$$L_{atm} = k_2 \cdot \frac{E_h}{V_m} \ , \tag{3}$$

where k_2 is a constant, E_h is the horizontal illuminance expressed in lux, and V_m is the meteorological visibility (visual range) expressed in meters. Also the E_h and V_m values could be estimated from measured or tabulated data [2]. However, a typical sunny day L_{atm} value is in general lower with respect to the L_{seq} value. Moreover, the E_h and V_m measurement procedures indicated by the UNI 11095 standard are quite bulky and complex, thus the L_{atm} is usually estimated from the tabulated data.

As a result, the key quantity for the L_v estimation is the equivalent veiling luminance L_{seq}. In order to easily estimate the L_{seq} value, the UNI 11095 standard provides a polar

978-1-4244-7935-1/11/$26.00 ©2011 IEEE

diagram similar to the one depicted in Fig. 1. Then, observing the tunnel from an height to the ground of 1.5 m, a distance to the tunnel equal to the stopping distance SD [2] and making the centre of the polar diagram overlap with the tunnel portal, the L_{seq} value could be estimated as [2]:

$$L_{seq} = k_1 \cdot \sum_{i=1}^{9} \sum_{j=1}^{12} L_{ij} \ , \tag{4}$$

where k_1 is a constant, i and j are the indexes of rings and sectors respectively, and L_{ij} is the average luminance emitted by the j^{th} sector of the i^{th} ring.
Also the L_{ij} values of (4) could be estimated from tabulated data or measured. The tabulated values of luminance for various typical surfaces are provided by empirical studies (CIE 88-1990 [3]), and are understood to represent with a sufficient frequency of time during the year for most common tunnel conditions. Hence, exploiting the tabulated L_{ij} values allows statistically providing safety for the drivers and avoiding energy wasting and unjustified higher lighting-costs. Nevertheless, it is straightforward to observe that sunny or cloudy days may result in safety reduction or energy wasting and higher lighting-costs respectively. Consequently, from any point of view the measurement of the L_{ij} values may provide better lighting performances.

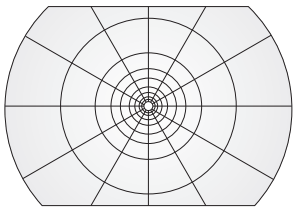

Fig. 1. Polar diagram similar to the one provided by UNI 11095 standard for the L_{seq} estimation process. Such as the UNI 11095 standard polar diagram, it is composed of 9 rings each one divided in 12 sectors; the outer sector subtending an angle of about 28° with the apex at the position of the eye of an approaching driver distant SD and aimed at the centre of the tunnel entrance. The diagram is pruned in order to take into account the stop effect provided by the vehicle windscreen.

III. Theoretical background and the proposed measurement method

From (4) it is straightforward to observe that the L_{seq} estimation requires the estimation of any of the L_{ij} luminances.

Actually, even considering a cosine corrected system – a system responding equally to radiation at any point across its surface and from any angle θ – the L_{seq} may not be directly estimated using a simple photodiode. This is due to the fact that the sectors areas of the polar diagram used in (4) are not constant, thus the equivalent veiling luminance L_{seq} is, in general, not directly proportional to the average object luminance, but the luminances relative to different sectors have to be differently weighted for the L_{seq} estimation.

The easiest way to differently weigh different object area is to exploit a camera system. Therefore, the proposed veiling luminance measurement method is based on a camera system. Hence, in the following three reference systems are used: the world coordinates (x, y, z) relative to the objects, the camera coordinates (x', y', z') relative to the image and, the pixel coordinates (c, r) – c and r are the row and column indexes respectively – relative to the photosensors array. In such coordinate systems, the x' axis is aligned with the optical axis of the camera system, θ is angle of incident light to the system optical axis and the distances of the object from the objective front focal point and of the image from the back focal are referred with d and d' respectively.

The analysis of relation between the object luminance $L(x, y, z)$ and the relative grey level $g(c, r)$ provided by a monochrome camera could be divided into two steps, thus analysing the relation between the luminance $L(x, y, z)$ of the object and the illuminance $E'(y', z')$ of the image on the image-plane first. Then, analysing the relation between the $E'(y', z')$ impinging on the photosensor array and the relative grey level $g(c, r)$.

An optical system can be properly approximated as a linear shift invariant system. Therefore, it can be described by a point spread function (psf) and the illuminance on the image plane is given by convolving the object luminance projected onto the image plane with the psf [4]. Hence, there is a biunique correspondence between the $L(x, y, z)$ and $E'(y', z')$ quantities.
Under far field condition ($d \gg f$, $d' \ll f$; being f the focal length of the optical system), the illuminance $E'(y', z')$ on the image plane developed by a Lambertian radiator having luminance $L(x, y, z)$ could be approximated as [4]:

$$E'(y', z') = T \cdot \pi \left[\frac{L(x, y, z)}{(f/_{\#})^2} \right] \cdot \cos^4 \theta \ , \tag{5}$$

where $f/_{\#}$ is the f-number of the optical system. Hence, the object luminance could be easily estimated from the image illuminace regardless to the actual object distance d.

On the other hand, the illuminance $E'(y', z')$ at the image plane is revealed by a suitable sensor (usually CCD) and converted into an electrical signal at discrete positions. Therefore, using the pixel coordinates (c, r), the relation between $E'(y', z')$ collected by the considered photosensor (r, c), and the provided grey level $g(c, r)$ – the digital number – is [4]:

$$g = t \int_{y'-\frac{1}{2}\Delta y'}^{y'+\frac{1}{2}\Delta y'} \int_{z'-\frac{1}{2}\Delta z'}^{z'+\frac{1}{2}\Delta z'} \int_{\lambda_1}^{\lambda_2} R_\lambda(\lambda) \cdot E'_\lambda(y', z') \, \mathrm{d}\lambda \mathrm{d}z' \mathrm{d}y' \ , \tag{6}$$

where, c and r are the indexes of the considered pixel, $\Delta y'$ and $\Delta z'$ are the pixel horizontal and vertical dimensions respectively, $[\lambda_1, \lambda_2]$ is wavelength range of the image illuminance, E'_λ is the image spectral illuminance, $R_\lambda(\lambda)$ is the digital sensor spectral responsivity relative to the (r, c) pixel and t is the exposure time. Equation (6) has been obtained considering an array composed of identical photosensor – $R_\lambda(y', z', \lambda) = R_\lambda(\lambda)$ –, neglecting any noise and supposing that the image illuminance $E'(y', z', \lambda)$ (the object luminance $L(x, y, z, \lambda)$) did not change during the exposure time t.

Concluding, from (5) and (6), $g(c, r)$ is proportional to $E'(y', z')$, thus to the $L(x, y, z)$. However, even though

$R_\lambda(r, c, \lambda)$ is with good approximation usually the same for all the pixel composing the CCD array [4], the photosensors responsivity $R = g/E'$ is generally known with high uncertainty. Moreover, from (5), it is straightforward to observe that the image generated by a spatially-constant luminance Lambertian radiator falls off with $\cos^4\theta$. Since the value of $\cos^4\theta$ falls rapidly as the angle θ increase, lens objective system are designed to partially compensate the marginal image illuminance reduction due to the $\cos^4\theta$ law [5]. Thus calibration of the camera systems is usually required.

It is important to notice that, even though the UNI 11095 standard did not define the maximum admissible measurement uncertainty, the accuracy required for the L_{seq} estimation process is implicitly low. As a matter of fact, as previously stated, the L_{seq} estimation may also be based on tabulated data, thus allowing high-uncertainty estimation. Moreover, in a wide range of luminance values, humans can not resolve relative luminance differences lower than 2% [4].

IV. The developed measuring system

The polar diagram of Fig. 1 and the calculation method reported in (4) are intended to provide an estimation of the average luminance contained in a conical field of view analogous to the one of an approaching driver, thus the camera system CS has to be designed in order to provide a field of view as close as possible to one shown in Fig. 1. Then, from (5) and (6), it is straightforward to observe that a biunique relation exist between the object luminance $L(x, y, z)$, the image illuminance $E'(y', z')$ and the grey level $g(c, r)$ provided by a monochrome camera. Hence, the veiling luminance L_{seq} may be easily estimated by analysing the image/s provided by a calibrated camera system. It is important to notice that the L_{seq} estimation process described by (4) is interested in the average object-sectors luminance L_{ij} only, thus resulting quite insensitive to blurring, geometric distortion and optical aberrations. Therefore, also low-cost optical components could be exploited for the development of the veiling luminance measuring instrument. As a result, the proposed measuring system is simply composed by a camera system (CS) connected to a personal computer aimed at analyzing the obtained images according to both the polar diagram shown in Fig. 1 and (4).

A. The camera system

Preliminary measurements have been performed exploiting a FireWire monochrome camera (model DMK 21AF04, The Imaging Source, Germany). The DMK 21AF04 camera uses a $1/4''$ CCD solid-state image sensor (model ICX098BL, Sony, Japan) with a square pixel array (CCD diagonal dimension equal 4.5 mm), thus a $f = 4$ mm focal length objective (T 0412 FICS-3, , The Imaging Source, Germany) has been chosen in order to obtain a field of view (f.o.v.) analogous to the one shown in Fig. 1. A picture of the camera system (DMK 21AF04 FireWire monochrome camera and T 0412 FICS-3 objective) is shown in Fig. 2.

In order to reduce the system sensitivity to the NIR (near infrared) spectral components, a UV-IR-CUT optical filter (model 486, The Imaging Source, Germany) has been placed in front of the T 0412 FICS-3 objective, thus giving rise to the overall camera system CS.

Even thought, the L_{seq} estimation process is quite insensitive to blurring, the minimum object distance d_{min} for an aberration-free optical system could be roughly estimated as [4]:

$$d_{min} \approx \frac{f^2}{2 \cdot f/_{\#} \cdot \epsilon} = \frac{(4 \cdot 10^{-3}\text{m})^2}{2 \cdot 1.2 \cdot 5.6 \cdot 10^{-6}\ \text{m}} \approx 1.2\ \text{m}\ , \quad (7)$$

where ϵ is the CCD square-pixel lateral dimension. Being the stopping distance SD of the order of tens of meters, the developed CS is able to properly image the tunnel scene.

Normally, the object is not a monochromatic radiator, thus the image. Therefore, in order to perform an estimation of the object luminance, the overall spectral responsivity $R_{\lambda\text{-}TOT}(\lambda)$ of the CS (optics, filter and photodetector) has to be as close as possible to the photopic CIE Standard Observer function $V(\lambda)$ [4], [6], [7]. Actually, monochrome camera systems (optics and CCD detector) are designed in order to provide grey levels that represent the objects as close as possible as they would have been seen by an observer. Moreover, as previously stated, the L_v estimation process does not require high accuracy, thus allowing us to arbitrary suppose that the CS spectral responsivity $R_{\lambda\text{-}TOT}(\lambda)$ perfectly match the $V(\lambda)$ curve shape. Obviously, no photometers can be matched perfectly to the $V(\lambda)$ function. Nevertheless, the degree of the spectral mismatch with the $V(\lambda)$ function may be evaluated by the term f_1' given in the CIE Publication 69 [8] (the term f_1' is an evaluation index and cannot be used for correction purposes).

B. Camera settings

It is straightforward to observe that the image illuminance $E'(y', z')$ is influenced by the objective settings even under the far field condition ($d \gg f$, $d' \ll f$) of (5). As a result, before starting the calibration activities, the objective focusing and iris aperture have to be properly set.

Because the CS has to be placed at a distance to the tunnel equal to the stopping distance SD, the focusing has been set in order to obtain a working distance similar to the stopping distance SD (about 120 m) (depth of field at least from SD to infinity).

The iris aperture has been set in order to avoid the CCD photosensor saturation. The used DMK 21AF04 camera allows exposure time t ranging from 2^{-13} s to 2^5 s. Therefore, in order to choose the proper iris aperture, the exposure time was set to 2^{-12} s and the iris aperture has been empirically set as maximum aperture that avoids both grey level saturation and blooming once the system was exposed to direct summer-sunlight. As shown in Fig. 2, a plastic ring has been added in order to both fix the objective settings and reduce the stray-light effects.

(a)

(b)

Fig. 2. The used camera system. It is composed by the DMK 21AF04 FireWire monochrome camera and T 0412 FICS-3 objective. As shown in (b), a grey plastic ring has been added in order to fix the objective settings. The plastic holder allows fixing the UV-IR-CUT optical filter also.

V. The proposed calibration method

Calibration of imaging system requires a luminance standard – homogeneous calibrated light source – or a reference calibrated imaging system; our calibration method makes use of a measurement standard.

A luminance standard is traditionally established using a diffuse reflectance or transmittance standard – opal glass, integrating sphere or reflectance standard – and a luminous intensity standard lamp.

Opal glass, illuminated by a known level of illuminance, has been the most widely used luminance standard because of its low cost, long-term stability, and ease of handling [7]. Despite the simplicity of the device, accurate measurements with an opal glass are complicated since it is sensitive to stray light from both sides of the glass and extreme care should be taken to minimize ambient reflection from the front and the back sides [7]. Moreover, an opal glass should be carefully uniformly illuminated over its entire surface area [7].

On the other hand, integrating sphere may establish a luminance standard with less uncertainty and difficulty than the traditional method using a diffuse reflectance or transmittance standard [7]. As a matter of the fact, imaging sensors are usually calibrated using integrated spheres [4], [9]. However, integrating spheres are expensive (about few thousands euros), thus not fulfilling the low-cost calibration method requirement. Hence, the CS has been calibrated by using a certified Lambertian diffuser reflectance standard LRS (model SRS-99-020, Labsphere, USA) (cost about two hundreds euros).

A. The calibration method

As previously reported, given the camera system CS, fixed the objective settings and under the far field condition ($d \gg f$, $d' \ll f$), the grey level $g(c,r)$ is biuniquelly related to the object luminance $L(y,z)$.

Actually, for the dark part of the image, the relative luminance resolution of a CCD system is usually lower than that of human eyes, thus video cameras generally convert the impinging illumination E' not linearly, but with some nonlinear functions such as the *Gamma correction* or the *Logarithmic transform* [4]. Obviously, such nonlinear functions routine have to be disabled in order to properly estimate the L_{seq}.

As previously reported in section II, the relation between the measurand $L(x,y,z)$ and the system output $g(r,c)$ depends on both the optics of the system (5) and the pixel responsivity (6), thus theoretically requiring the estimation of the responsivity of any of the pixels composing the CCD array. Actually, CCD arrays show a certain degree of nonuniform response of individual pixels, which could be described by two terms: different dark signal (fixed pattern noise, FNP) and a different responsivity (photoresponse nonuniformity, PRNU) [4]. However, FPN is generally remarkably low (about 0.04% of the full grey value range), and PRNU is also very low (typically the responsivity standard deviation is about 0.3%) [4]. As a result, the shape of the calibration diagram is mainly determined by the residual $\cos^4\theta$ behaviour, hence it is not necessary to estimate the responsivity of any of the pixels composing the CCD array.

The geometry of the used calibration method is shown in Fig. 3. The LRS was uniformly illuminated by a 75 W xenon lamp system (model 6251, Oriel, USA) at nominal normal incidence, and the illuminance E_0 on the diffuser surface was measured using a reference photometer (model HD 9221, Delta OHM, Italy). As shown in Fig. 3, the CS was placed at a 45° angle with respect to the diffuser LRS, thus avoiding collecting the specular reflection components of real Lambertian diffusers [7].

Then, the object luminance L was simply estimated as [4], [6]:

$$L = \frac{\rho \cdot E_0}{\pi} \ , \tag{8}$$

where $\rho = 0.9880 \pm 0.005$ is the LRS-diffuser average reflectance-factor in the visible range.

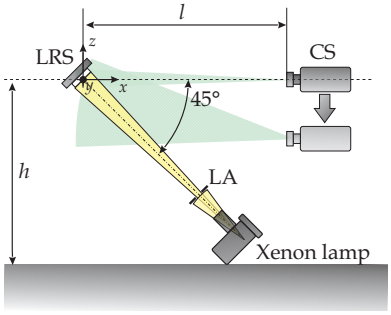

Fig. 3. Experimental setup used for the calibration activities. The LRS was illuminated by the xenon lamp that provides an uniform illuminance E_0 onto the Lambertian diffuser surface. The limiting aperture LA allows illuminating the LSR only, thus reducing the stray-light collected by the CS. The CS was moved in the (y,z) plane, thus allowing calibrating the CS for different object positions.

On the other hand, the grey level was assessed by a spatial

average. Hence, in order to reduce the noise due to: i) the xenon-lamp illuminance E_0 and LRS reflectivity spatial inhomogeneities and, ii) small dirt particles on the objective, the cover glass of a CCD sensor and the IR cutoff filter, the grey level was estimated performing a "spatial-average" on a CCD area of about $\Delta_c \cdot \Delta_r$ pixels, thus giving rise to spatial-average grey level $g_{s-m}(c_0, r_0)$:

$$g_{s-m}(c_0, r_0) = \frac{1}{\Delta_c \cdot \Delta_r} \cdot \sum_{c=c_0-\frac{1}{2}\Delta c}^{c_0+\frac{1}{2}\Delta c} \left[\sum_{r=r_0-\frac{1}{2}\Delta r}^{r_0+\frac{1}{2}\Delta r} g(c, r) \right] , \quad (9)$$

where (c_0, r_0) are the coordinates of the centre of the considered rectangular area.
Then, in order to reduce the noise due to: i) the CCD, ii) the reference photometer used for the E_0 estimation and, iii) temporal fluctuation the of xenon-lamp illuminance E_0, the obtained g_{s-m} values were averaged over N_f frames, thus giving rise to the temporal-average grey level g_{t-m}:

$$g_{t-m}(c_0, r_0) = \frac{1}{N_f} \cdot \sum_{i=1}^{N_f} g_{s-m}^{(i)} , \quad (10)$$

where, $g_{s-m}^{(i)}(c_0, r_0)$ is the $g_{s-m}(c_0, r_0)$ value relative to the i^{th} aquired frame.
Finally, for all the investigated L values ranges, the exposure time t was set in order to virtually exploit the full grey value range without reaching the sensor saturation, thus further reducing the CCD noise [4].

B. Results

Activities have been performed accordingly to the calibration method previously described in subsection V-A.
Even though the responsivity of photometers is known to change depending on the temperature of their components, the environmental temperature was neither controlled nor measured. Nevertheless, both the CS, the reference photometer and the xenon lamp system have been set up in its measurement location with their power turned on for at least 1 h before measurements.
In order to satisfy the far field condition and reduce blurring, the LSR has been placed at a distance l of about 150 cm from the CS. As shown in Fig. 4, the CS was moved in the (y, z) plane, thus obtaining the formation of the LRS image on different positions of the CCD detector. The grey levels relative to the LRS image displayed in Fig. 4 are shown in Fig. 5.

As an example, Table I reports the estimated CS responsivity R_{TOT-e} for different object position. According to subsection V-A, the estimation of the LRS luminance L has been performed by means of (8).
On the other hand, the grey levels have been assessed by a tempo-spatial average. The grey levels $g_{s-m}^{(i)}$ have been estimated performing a spatial-average on a CCD area of about $\Delta_c = 20$ and $\Delta_c = 10$ pixels. Then, they have been averaged over $N_f = 100$ frames, thus obtaining the temporal-average grey levels $g_{t-m}(c_0, r_0)$. In order to further reduce the CCD noise, the CCD exposure time t was experimentally set to fully

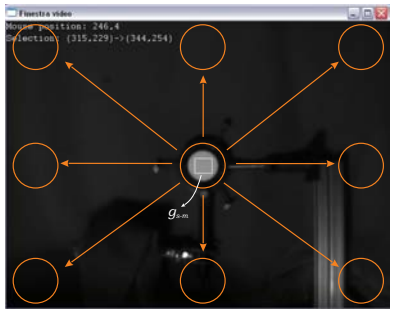

Fig. 4. Snapshot acquired using the CS; the picture has been obtained with a CS to LRS distance $l \approx 100$ cm and tilting the LRS orthogonal to the CS optical axis. As shown in Fig. 3, moving the CS it is possible to calibrate different points. The white-line rectangle overlapped to the LRS image, underlines the pixels considered in the spatial-average grey level (g_{s-m}) estimation.

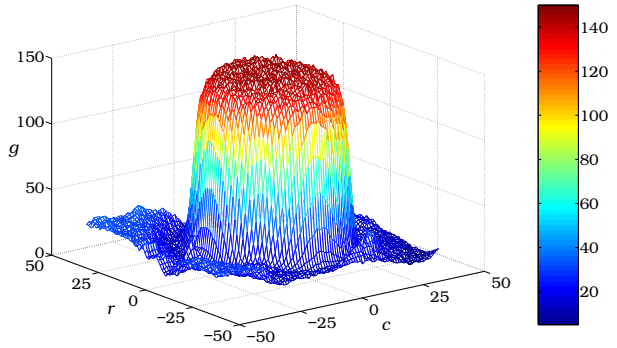

Fig. 5. Grey levels relative to the LRS image displayed in Fig. 4. In the (c, r) pixel coordinates system, the $(0, 0)$ coordinate refers to the center of the CCD.

exploiting the dynamic range (grey value) without reaching the sensor saturation ($t = 2^{-6}$ s).
From (8), the R_{TOT-e} has been estimated as:

$$R_{TOT-e}(c_0, r_0) = \frac{g_{t-m}(c_0, r_0)}{\rho \cdot \bar{E}_0 / \pi} , \quad (11)$$

where $\bar{E}_0$ is the mean of the $N_{E_0} = 3$ E_0-values recorded during the acquisition of the N_f frames relative to the considered $g_{t-m}(c_0, r_0)$:

$$\bar{E}_0 = \frac{1}{N_{E_0}} \sum_{i=1}^{N_{E_0}} E_0 . \quad (12)$$

Of course, the R_{TOT-e} values are affected by uncertainty. Thus, the combined standard measurement uncertainties associated to the R_{TOT-e} values have been estimated applying the analytical procedure suggested by the International Standardization Organization [10] to (11). The considered sources of uncertainty have been: the uncertainty associated with both the LRS average reflectance-factor and the HD 9221 photometer, and the experimental standard deviation of the g_{s-m}, g_{t-m} and $\bar{E}_0$ quantities.
Table I reports the R_{TOT-e} values and the relative estimated standard uncertainty.

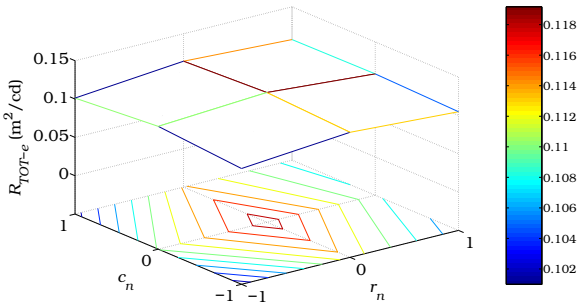

Fig. 6. Nine-points calibration diagram obtained using the calibration method described in subsection V-A. In the normalized c_n and r_n pixel coordinates system, the $(0,0)$ coordinate refers to the centre of the CCD, whereas the -1 or 1 coordinate refers to the CCD boundaries.

TABLE I

ESTIMATED R_{TOT-e} VALUES EXPRESSED IN (m^2/kcd). IN THE NORMALIZED c_n AND r_n PIXEL COORDINATES SYSTEM, THE $(0,0)$ COORDINATE REFERS TO THE $\Delta_r \cdot \Delta_c$ PIXEL AREA IN THE CENTRE OF THE CCD, WHEREAS THE -1 OR 1 COORDINATE REFERS TO THE CCD BOUNDARIES. THE R_{TOT-e} VALUES HAVE BEEN OBTAINED USING A PIXELS AREA $\Delta_c \cdot \Delta_r$ EQUALS TO 20X10, A NUMBER OF FRAMES N_f EQUAL TO 1000, AND AN EXPOSURE TIME t EQUAL TO 2^{-6} S.

	$c_n = -1$	$c_n = 0$	$c_n = 1$
$r_n = -1$	101.00 ± 4.4%	113.09 ± 4.4%	104.81 ± 4.3%
$r_n = 0$	110.02 ± 4.4%	119.17 ± 4.4%	108.32 ± 4.4%
$r_n = 1$	101.28 ± 4.3%	114.22 ± 4.4%	107.27 ± 4.4%

VI. DISCUSSION AND CONCLUSIONS

In road-tunnels lighting field, the real-time measurement of the veiling luminance may allow the estimation of the optimum luminance levels, thus increasing the drivers safety and avoiding energy wasting and unjustified higher lighting-costs or driver dazzle.

In this paper, we propose a low-cost system and calibration method for veiling luminance estimation. The calibration cost may be probably further reduced by using lower cost camera. Although, the light-source-cost is common to opal glass and integrating sphere methods also, cheaper light sources such as halogen lamp may be used. As a matter of the fact, under the (optimistic) hypothesis that the CS spectral responsivity $R_{\lambda-TOT}(\lambda)$ perfectly matches the $V(\lambda)$ curve shape, the calibration process results insensitive to the actual lamp colour temperature. Moreover, also cheaper Lambertian diffuser – white paper – may be used. However, the estimation of the reflectance factor ρ of the uncalibrated reflectance standard may result in a non-trivial task.

Actually, most surfaces display a combination of specular and diffuse behaviour, with the specular becoming increasingly noticeable for large angles of incidence and observation (measured from the surface normal), which is particularly the case for road surfaces [11]. Although the proposed calibration activities have been performed by using a Lambertian-diffuser reflectance standard (LRS), the developed measuring system is only little affected by the actual optical behaviour of the imaged objects. Such is due to the fact that the CS has been designed in order to provide a f.o.v. analogous to the one of Fig. 1, thus, in turn, analogous to the one of an approaching driver. As a result, the calibrated CS collects almost the same luminance as it will be collected by the approaching driver. Calibration activities make use of a LRS simply because its luminance may be easily estimated using (8).

ACKNOWLEDGMENT

The authors wish to thank Andrea Nosari for his contribution during the experimental activities.

REFERENCES

[1] *Lighting applications - Tunnel lighting, CR 14380:2003*, CEN/TC 169 - Light and lighting, Brussels, Belgium, 2003.

[2] *Luce e illuminazione: Illuminazione delle gallerie*, UNI, Ente Nazionale Italiano di Unificazione, Milan, Italy, 2003.

[3] *Guide for the lighting of road tunnels and underpasses*, CIE, Commision Internationale de l'Eclairage, Vienna, Austria, 1990.

[4] B. Jähne, *Practical handbook on image processing for scientific and technical applications*, 2nd ed. CRC Press, 2004.

[5] N. Asada, A. Amano, and M. Baba, "Photometric calibration of zoom lens systems," *Pattern Recognition, 1996., Proceedings of the 13th International Conference on*, vol. 1, pp. 186–190, Aug 1996.

[6] E. F. . Zalewski, *Radiometry and Photometry*, 2nd ed., ser. Handbook of optics. McGraw-Hill, 1995, vol. 2, ch. 24.

[7] Y. Ohno, *Photometric Standards*, ser. Handbook of Applied Photometry. Optical Society of America and Springer-Verlang, 1997, ch. 3.

[8] *Methods of characterizing illuminance meters and luminance meters, CIE 69:1987*, CIE, Commision Internationale de l'Eclairage, Vienna, Austria, 1987, ISBN: 978 3 900734 04 6.

[9] S. W. Brown, T. C. Larason, C. Habauzit, G. P. Eppeldauer, Y. Ohno, and K. R. Lykke, "Absolute radiometric calibration of digital imaging systems," M. M. Blouke, J. Canosa, and N. Sampat, Eds., vol. 4306, no. 1. SPIE, 2001, pp. 13–21. [Online]. Available: http://link.aip.org/link/?PSI/4306/13/1

[10] *Guide to the Expression of Uncertainty in Measurement*, ISO, Int. Org. Standardization, Geneva, Switzerland, 1995.

[11] *Road transport lighting for developing countries, CIE 180:2003*, CIE, Commision Internationale de l'Eclairage, Vienna, Austria, 2007, ISBN 978 3 901906 61 9.